



Organo-peroxyl compounds via catalytic oxidation of a hindered phenol and aniline utilizing new manganese(II) bis benzimidazole diamide based complexes

Ruchi Bakshi, Pavan Mathur*

Department of Chemistry, University of Delhi, Delhi, India

ARTICLE INFO

Article history:

Received 3 July 2009

Received in revised form 28 June 2010

Accepted 30 June 2010

Available online 13 July 2010

Keywords:

Manganese(II)

Benzimidazole diamides

Hydroperoxides

Tri-tert.-butylphenol

Tri-tert.-butylaniline

ABSTRACT

Bis benzimidazole diamide ligand-*N,N'*-bis(2-methylbenzimidazolyl) propanediamide [GBMA = L] has been synthesized and utilized to prepare new Mn(II) complexes of general composition $[Mn(L)X_2] \cdot nH_2O$ where X is an exogenous anionic ligand ($X = Cl^-$, CH_3COO^- , SCN^-). The geometry of the ligand and its Mn(II) complex have been optimized at the level of UHF, by using ZINDO/1 method. Binding energies, heat of formation and bond lengths of geometry optimized structures for the ligand and complex have been obtained. The oxidation of 2,4,6-tri-tert.-butylphenol (TTBP) and 2,4,6-tri-tert.-butylaniline (TTBA) has been investigated using these Mn(II) complexes as catalyst and TBHP as an alternate source of oxygen. The organo-peroxyl compounds have been isolated and characterized by 1H NMR, ^{13}C NMR, IR and mass data. A different product profile was obtained when H_2O_2 is used as an oxidant.

© 2010 Elsevier B.V. All rights reserved.

1. Introduction

Mononuclear Mn(II) coordination compounds have been studied due to their importance in material chemistry, catalysis and biological chemistry and they are often used for the development of catalysts especially for oxidation reactions [1]. The reactivity of such Mn(II) complexes has been correlated with their electronic properties and hence geometric structure [2–5].

Oxidation of phenols is a relatively facile reaction which may be carried out with various oxidants. However, such procedures are often non-selective, giving rise to a very complex mixture of products [6]. The catalytic oxidation of substituted phenols and anilines has also proved to be a useful procedure for mechanistic studies [6–8]. In earlier attempts the effect of different central atoms (Co, Mn) and various chelating ligands (schiff bases, porphyrins, oximes) on the catalytic activity and the product distribution has been investigated [9]. In this context, several authors have utilized hindered phenols as substrates for oxidation reactions. Kitajima et al. [10] and Gupta and Mukherjee [11] have reported both coupled diphenoquinones and bisphenols using a binuclear copper complex, while Gupta et al. [12] have reported formation of benzoquinones from oxidation of 2,4,6-tri-tert.-butylphenol, utilizing Cu(II) complexes in the presence of molecular oxygen.

The present study reports the oxidation of a hindered phenol/aniline utilizing Mn(II) complexes as catalysts and with low

concentration of the oxidant. Further the difference in the product profile has been studied by using two different oxidants, while keeping the catalyst fixed. The activity of Mn(II) complexes as catalysts in terms of stability of higher oxidation state has also been probed.

2. Experimental

2.1. Materials and methods

Glycine benzimidazole dihydrochloride was prepared following the procedure reported by Cescon and Day [13]. Freshly distilled solvents were employed for all synthesis work. Spectroscopic grade solvents were employed for spectral experiments. All other chemicals were of AR grade. 2,4,6-Tri-tert.-butylphenol (TTBP), and 2,4,6-tri-tert.-butylaniline were procured from Sigma Aldrich. TTBP was twice recrystallized from $CH_3OH:H_2O$ mixture. Tert.-butylhydroperoxide (TBHP) was introduced slowly to minimize disproportionation of the peroxide that may be catalyzed by the manganese complexes. Elemental analyses were obtained from micro-analytical laboratory of RSIC, Chandigarh, India. Electronic spectra were recorded on a Shimadzu UV-1601 Spectrophotometer at the Department of Chemistry, University of Delhi, Delhi, India. IR spectra were recorded in the solid state as KBr pellets on a Perkin-Elmer FTIR-2000 Spectrometer (IR stretching frequencies measured to an accuracy of $\pm 1 \text{ cm}^{-1}$). 1H NMR and ^{13}C NMR spectra were recorded on a 300 MHz Bruker-Spin instrument at the Department of Chemistry, University of Delhi and at IIT-Delhi,

* Corresponding author.

E-mail address: pavanmat@yahoo.co.in (P. Mathur).

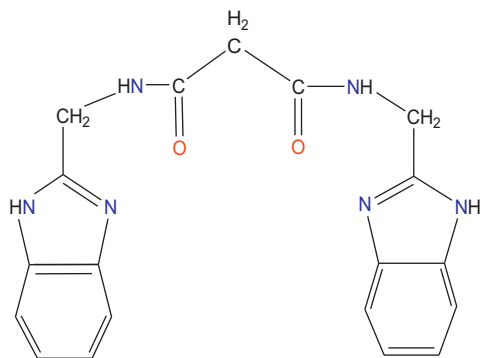
Delhi, India. Cyclic Voltammetric measurements were carried out on a BAS-CV 50W electrochemical analysis system. Cyclic voltammograms of all the complexes were recorded in DMSO solution with 0.1M TBAP as a supporting electrolyte. A three electrode configuration composed of a Pt-disk working electrode, a Pt wire counter electrode and an Ag/AgNO₃ reference electrode was used for measurements. The reversible one-electron Fc/Fc⁺ couple has an $E_{1/2}$ of 0.145 V versus an Ag/AgNO₃ electrode. The electro spray mass spectra were recorded on a MICROMASS QUATTRO II triple quadrupole mass spectrometer at CDRI, Lucknow, India. Solid state EPR spectra were recorded on the X-Band on a Bruker-spectrospin at IIT-Bombay, Mumbai, India.

2.2. Synthesis

2.2.1. *N,N'*-Bis(2-methylbenzimidazolyl)-propanediamide [GBMA][L]

A solution of glycine benzimidazole dihydrochloride (5.0 g, 22.8 mmol) in pyridine (10 ml) was added to a solution of malonic acid (1.2 g, 11.4 mmol) in pyridine (5 ml). The mixture was stirred gently for 10 min, during which a white precipitate appeared. The reaction mixture was then heated slowly on a water bath at a temperature of 45 °C and to it triphenylphosphite (5.9 ml, 22.8 mmol) was added dropwise over a period of 15 min. The reaction mixture was simultaneously stirred. After addition of P(OPh)₃ was complete and the initially formed white precipitate dissolved, the temperature of the reaction mixture was slowly raised to 75 °C and the clear solution was stirred for 6–7 h. A white solid resulted which was filtered off, washed with chloroform and neutralized. The crystalline product so obtained was recrystallized with EtOH/H₂O (1:1) mixture and analyzed for composition C₁₉N₆O₂H₁₈·3H₂O

Anal. Calc.: C, 54.8; H, 5.8; N, 20.2. *Found*: C, 53.9; H, 5.0; N, 19.5%. *M.p.*: 230 °C, *Yield*: 3.9 g (42%), IR (KBr pellets): 3485 (ν_{OH}), 3256 (ν_{NH amide}), 3092 (ν_{NH benzim}), 1629 (ν_{C=O amideI}), 1562 (ν_{C-N amideII}), 1444 (ν_{C=N-C=C- benzim}), 735 (ν_{C=C benzene ring vibration}), λ_{max}, nm (log ε): 274 (4.0), 280 (3.9), ¹H NMR (d₆-DMSO): 3.1 (s, 2H), 4.3 (d, 4H, *J* = 5.4 Hz), 6.9 (m, 4H), 7.2 (d, 2H, *J* = 6.8 Hz), 7.3 (d, 2H, *J* = 6.4 Hz), 8.6 (t, 2H, *J* = 5.1 Hz), 12.06 (s, 2H) (Fig. 1 – Supplementary material).



2.2.2. [Mn(L)X₂] where L = GBMA; X = Cl⁻, CH₃COO⁻

A methanolic solution (5 ml) of ligand L (0.3 mmol) was added to the methanolic solution (5 ml) of MnCl₂·4H₂O (0.3 mmol). The resulting light yellow coloured solution was stirred for 2 h. A white product precipitated which was filtered, washed with small amount of methanol and dried under vacuum over anhydrous CaCl₂. The compounds were analysed for the following compositions:

2.2.2.1. MnC₁₉N₆O₂H₁₈·Cl₂·3H₂O. *Anal. Calc.*: C, 42.1H, 4.4; N, 15.5. *Found*: C, 42.4; H, 4.3; N, 14.7%. *Yield (%)*: 98 mg (75%), IR (KBr pellets, cm⁻¹): 3495 (ν_{OH}), 3302 (ν_{NH amide}), 3187 (ν_{NH benzim}), 1636 (ν_{C=O amideI}), 1562 (ν_{C-N amideII}), 1454 (ν_{C=N-C=C- benzim}), 742 (ν_{C=C benzene ring vibration}), $E_{1/2}$ = +718 mV.

2.2.2.2. MnC₁₉N₆O₂H₁₈·(CH₃COO)₂·4H₂O. *Anal. Calc.*: C, 45.5; H, 5.2; N, 13.8. *Found*: C, 44.6; H, 5.0; N, 14.6%. *Yield (%)*: 91 mg (70%), IR (KBr pellets, cm⁻¹): 3410 (ν_{OH}), 3273 (ν_{NH amide}), 3021 (ν_{NH benzim}), 1642 (ν_{C=O amideI}), 1560 (ν_{C-N amideII}), 1425 (ν_{C=N-C=C- benzim}), 738 (ν_{C=C benzene ring vibration}), 1340 (ν_{acetate(symm)}), anodic potentials = +500 mV, +750 mV.

2.2.3. [Mn(L)(SCN)₂]; L = GBMA

A concentrated solution of potassium thiocyanate in methanol was added dropwise to a methanolic solution (5 ml) of MnCl₂·4H₂O (0.3 mmol) till KCl precipitated. This was centrifuged and the centrifugate was added to a methanolic solution (5 ml) of ligand (0.3 mmol). The mixture was stirred for 1 h when a creamish-white precipitate was obtained. This was filtered, washed with methanol and dried under vacuum over anhydrous CaCl₂. The complex was analyzed for the composition MnC₁₉N₆O₂H₁₈·(SCN)₂·3H₂O.

Anal. Calc.: C, 42.9; H, 4.1; N, 19.1. *Found*: C, 42.0; H, 4.1; N, 18.9. *Yield (%)*: 95 mg (68%), IR (KBr pellets, cm⁻¹): 3425 (ν_{OH}), 3299 (ν_{NH amide}), 3183 (ν_{NH benzim}), 1633 (ν_{C=O amideI}), 1526 (ν_{C-N amideII}), 1454 (ν_{C=N-C=C- benzim}), 741 (ν_{C=C benzene ring vibration}), 2041 (ν_{C=N}), 849 (ν_{S-C}), $E_{1/2}$ = +697 mV.

The presence of water molecules was determined by IR and TGA experiments.

2.2.4. Energy optimized structures of the ligand and the complex

The geometry of the ligand and its Mn(II) complex have been optimized at the level of UHF (Unrestricted Hartree-Fock) approach [14,15]. The geometry optimization of the structures was performed by using ZINDO/1 (Zerner Intermediate Neglect of Differential Overlap) method. The optimization was done successively and iteratively till the desired precision and consistency was achieved (the optimizations were obtained by the application of the Steepest Descent Method followed by Polak-Ribier algorithm consecutively with a conversion limit of 0.01 kcal mol⁻¹ and RMS gradient of 0.01 kcal mol⁻¹/Å°). The calculated values of the binding energy and the other electronic parameters are given under Section 3.

The optimized structures of the ligand and the complex L and Mn(II)-L (penta coordinated) are given in Fig. 2a and b (Supplementary material), respectively.

2.2.5. Oxidation of 2,4,6-tri-tert.-butylphenol (TTBP) and 2,4,6-tri-tert.-butylaniline (TTBA) using Mn(II) complexes and oxidants H₂O₂ (hydrogen peroxide) and TBHP (tert.-butylhydroperoxide)

A solution of TTBP (381 mM)/TTBA (127 mM) in 3 ml MeOH was prepared. A suspension of [Mn(L)Cl₂] complex (12.7 mM) in MeOH was added to the above solution followed by addition of H₂O₂ (381 mM for TTBP and 127 mM for TTBA). The above reaction was repeated by substituting H₂O₂ with TBHP as oxidant (381 mM for TTBP and 127 mM for TTBA). The reaction mixture was stirred for 48 h on a water bath at a temperature of 45 °C and was monitored continuously using TLC. 2 spots were observed at different R_f values. After 48 h, the reaction mixture was worked up on a short column, eluting with 20% ethyl acetate/hexane. Evaporation of the eluent to a small volume and keeping it overnight gave the desired product. The product with higher R_f could be isolated in sufficient yield (Table 1). Recovery and subsequent usage of the catalyst [Mn(L)Cl₂] was found to give decreased yields of the products. The product was further characterized by ¹H NMR (Fig. 3a–d), ¹³C NMR (Fig. 4a–d), mass spectrometry (Fig. 5a–d) and IR spectral studies. ¹³C NMR is in reference to similar products

Table 1

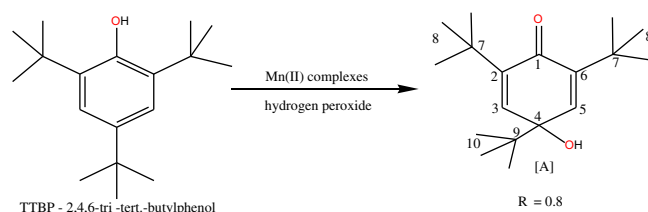
Turnover no. and % yield of the products.

Substrate	Oxidant	Turnover	% Yield
TTBP	H ₂ O ₂	10	49.09
TTBA	H ₂ O ₂	11	56.03
TTBP	TBHP	5	23.45
TTBA	TBHP	10	47.54

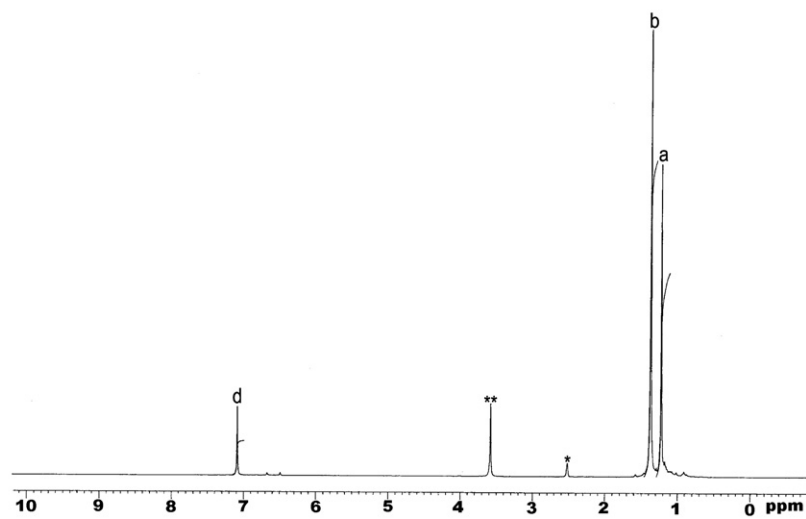
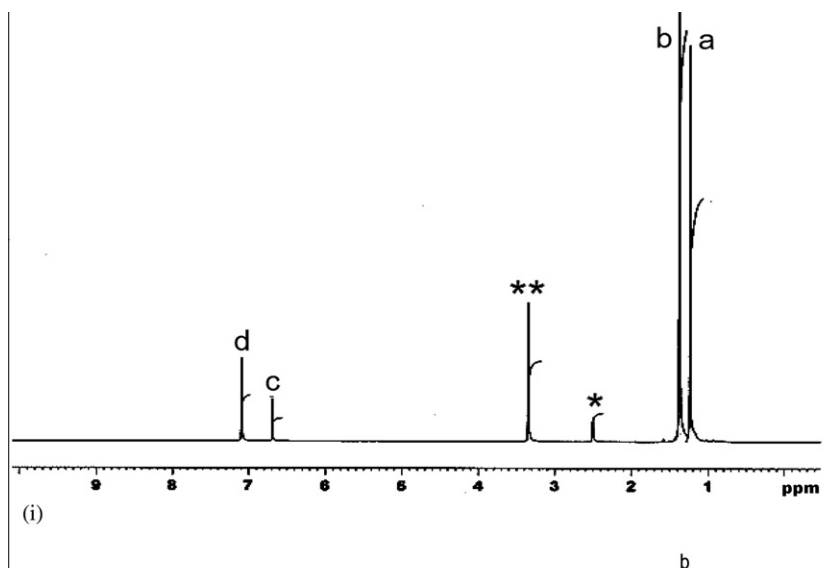
reported earlier [16]. The above studies support the formation of the products identified as 'A', 'B', 'C', 'D' as shown below.

The above oxidation reaction was also carried out by using [Mn(L)(CH₃COO)₂] as catalyst instead of [Mn(L)Cl₂]. Upon employing [Mn(L)(CH₃COO)₂] complex as catalyst, it was found that the product profile obtained was quite complex and column chromatography did not yield the separation of a single product. A comparison of the cyclic voltammograms of the two complexes gives a clue as to why a complex product profile was obtained. It is found that while a quasi-reversible wave with a $E_{1/2}$ of +718 mV is observed for the [Mn(L)Cl₂] complex, the acetate bound compound shows two anodic waves observed at 500 and 700 mV, respec-

tively, with no corresponding cathodic wave being observed. This suggests that the higher oxidation states of Mn(III) and Mn(IV) are highly oxidising and unstable in nature, in the acetate bound compound. This may also explain as to why multiple products were obtained while using [Mn(L)(CH₃COO)₂] as catalyst for oxidation of a hindered phenol and aniline.

(i) Oxidation of TTBP in presence of H₂O₂

¹H NMR (*d*₆-DMSO) (ppm): 1.19 (s, 9H), 1.37 (s, 18H), 6.69 (s, 1H), 7.09 (s, 2H) (Fig. 3a). ¹³C NMR (*d*₆-DMSO): 141.6 (C-2, C-6),



* = DMSO
** = moisture

Fig. 3a. (i) ¹H NMR in *d*₆-DMSO of oxidation product of TTBP with Mn(L)Cl₂ and H₂O₂ (ii) ¹H NMR in *d*₆-DMSO of oxidation product of TTBP with Mn(L)Cl₂ and H₂O₂ (D₂O exchange experiment).

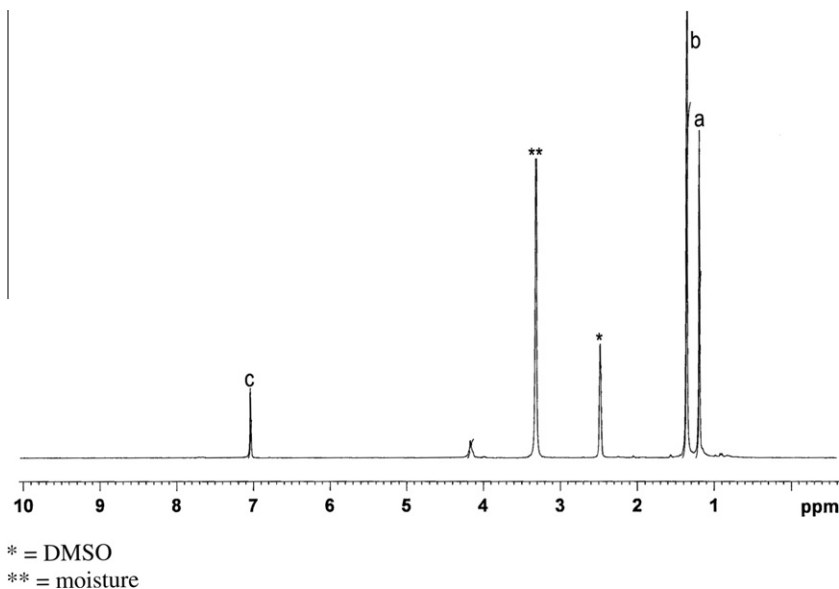
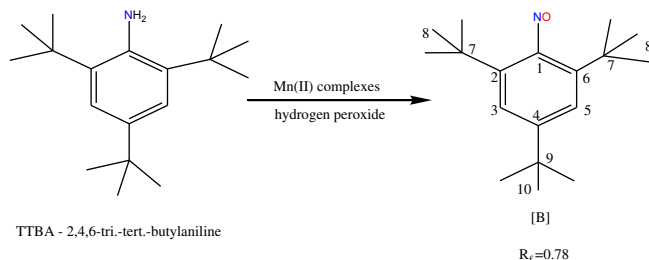


Fig. 3b. ^1H NMR in d_6 -DMSO of oxidation product of TTBA with Mn(L)Cl_2 and H_2O_2 .

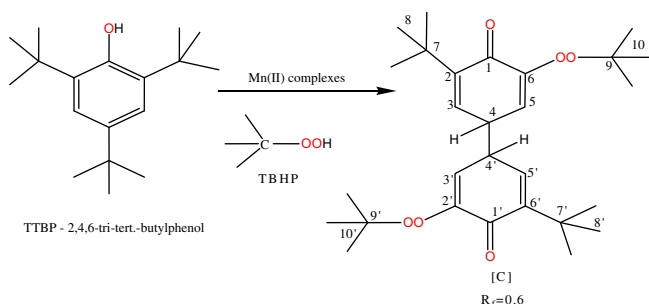
138.7 (C-3, C-5), 121.5 (C-4), 35.1 (C-7), 30.9 (C-8), 34.5 (C-9), 32 (C-10) (Fig. 4a). ESI MS^+ (m/e): 278, 262, 247, 222, 221 (Fig. 5a). IR (cm^{-1}): 3645, 1651, 1362, % yield: 55 (Yields refer to isolated yield).

(ii) Oxidation of TTBA in presence of H_2O_2



^1H NMR (d_6 -DMSO) (ppm): 1.22 (s, 9H), 1.38 (s, 18H), 7.06 (s, 2H) (Fig. 3b). ^{13}C NMR (d_6 -DMSO): 168.0 (C-1), 142.1 (C-4), 133.0 (C-2, C-6), 121.3 (C-3, C-5), 34.8 (C-7), 30.5 (C-8), 34.3 (C-9), 32.0 (C-10) (Fig. 4b). ESI MS^+ (m/e): 274, 261, 246, 230 (Fig. 5b). IR (cm^{-1}): 1620, 1363, % yield: 75 (Yields refer to isolated yield).

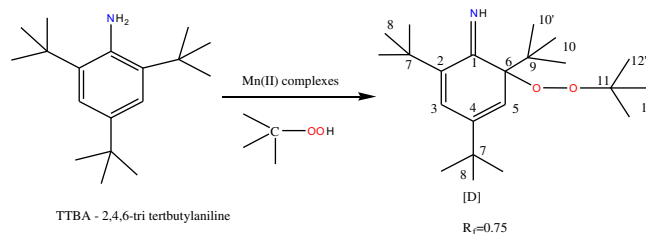
(iii) Oxidation of TTBP in presence of TBHP



^1H NMR (d_6 -DMSO) (ppm): 0.93 (s, 2H), 1.17–1.19 (m, 9H), 1.24 (s, 9H), 1.38 (s, 18H), 6.67 (s, 2H), 7.09 (s, 2H) (Fig. 3c). ^{13}C NMR (d_6 -DMSO): 188.0 (C-1), 141.2 (C-2), 138.2 (C-3), 141.0 (C-4), 121.2 (C-5), 79.0 (C-6), 34.3 (C-7), 31.5 (C-8), 81.9 (C-9), 26.9 (C-10), 185.9 (C-1'), 79.0 (C-2'), 121.2 (C-3'), 141.0 (C-4'), 129.9 (C-5'), 147.7 (C-6'), 33.8 (C-7'), 30.4 (C-8'), 81.9 (C-9'), 25.6 (C-10') (Fig. 4c). ESI MS^+ (m/e): 474, 432, 416, 400 (Fig. 5c).

IR (cm^{-1}): 1667, 1646, 1362, % yield: 42 (Yields refer to isolated yield).

(iv) Oxidation of TTBA in presence of TBHP



^1H NMR (d_6 -DMSO) (ppm): 1.17 (s, 9H), 1.22 (s, 9H), 1.25–1.27 (m, 9H), 1.33 (s, 9H), 6.61 (s, 1H), 7.06 (s, 1H) (Fig. 3d). ^{13}C NMR (d_6 -DMSO): 166.8 (C-1), 139.9 (C-2), 133.0 (C-3), 141.5 (C-4), 134.4 (C-5), 83.3 (C-6), 34.7 (C-7), 30.5 (C-8), 32.0 (C-9), 31.3 (C-10), 31.2 (C-10'), 79.2 (C-11), 26.8 (C-12), 25.9 (C-12') (Fig. 4d). ESI MS^+ (m/e): 350, 277, 220 (Fig. 5d).

IR (cm^{-1}): 1651, 1374, % yield: 50 (Yields refer to isolated yield).

3. Results and discussion

3.1. Description of energy optimized structure

The binding energy for the ligand L has been found to be $-15044.42 \text{ kcal mol}^{-1}$ and that of the Mn(II) complex is $-14824.73 \text{ kcal mol}^{-1}$. The heat of formation (H_f) are $-10062.55 \text{ kcal mol}^{-1}$ and $-9746 \text{ kcal mol}^{-1}$, respectively. In the optimized structure the benzimidazole rings are found to be nearly

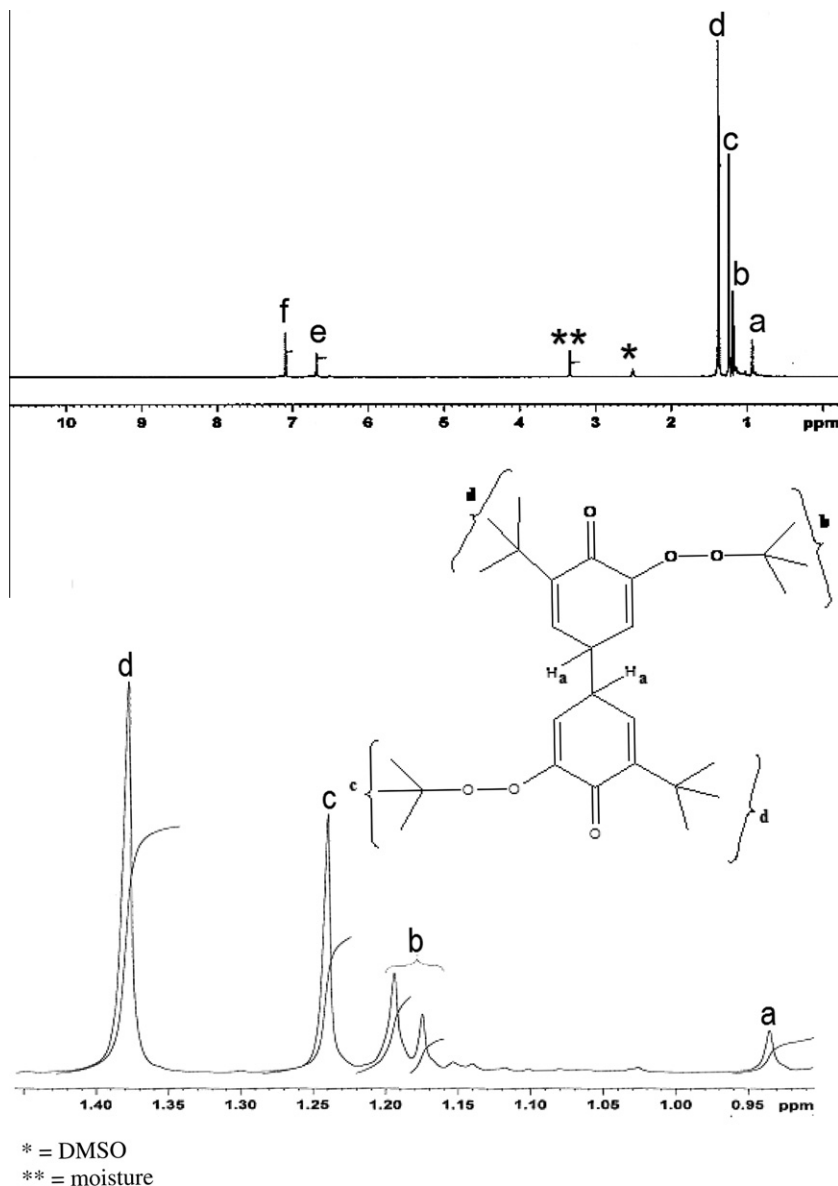


Fig. 3c. ^1H NMR in d_6 -DMSO of oxidation product of TTBP with $\text{Mn}(\text{L})\text{Cl}_2$ and TBHP and blow ups of relevant position.

perpendicular to one another, possibly minimizing the interactions between the rings. The bond lengths and IR bands of geometry optimized structures were compared with the structures for a similar diamide ligand and a five coordinated $\text{Cu}(\text{II})$ complex reported earlier [17,18], and it is found that there is a close correspondence, supporting the structures obtained after geometry optimization (Table 2a and b – Supplementary material).

3.2. Electronic spectroscopy and IR data

The electronic spectra of the ligand shows two strong bands in the UV region 273–284 nm. These bands are assigned to the $\pi-\pi^*$ transition characterizing the benzimidazole group.

The free ligand L has characteristic IR bands at 1629 cm^{-1} amideI ($\nu_{\text{C=O}}$), 1562 cm^{-1} amideII ($\nu_{\text{C=N}}$ amide), 1444 cm^{-1} ($\nu_{\text{C=N=C=N}}$ benzimidazole), respectively. On complexation a decrease in amideI and increase in amideII has been observed, which is in accordance with the coordination of the ligand through an amide carbonyl oxygen [18]. Thus, the manganese complexes have amide carbonyl coordination rather than amide NH coordination.

Characteristic stretching frequencies for the coordinated anions are also observed. Bands at 2041 and 849 cm^{-1} in the thiocyanate complex are assigned to $\nu_{\text{C=N}}$ and $\nu_{\text{C-S}}$ stretching of the thiocyanate group. This shows coordination of the thiocyanate group through the N atom. Similarly, the band at 1340 cm^{-1} in the acetate complex is assigned to monodentate bound acetate.

3.3. ^1H NMR Spectra

^1H NMR spectrum of the free ligand L shows signals for aliphatic and aromatic protons with theoretically predicted splittings. A signal is observed at 12.0 ppm corresponding to the N–H benzimidazole proton. Multiplets in the range of 7.1–7.8 ppm arise due to the benzimidazole ring protons characteristic of an AA'BB' pattern. The linker $-\text{CH}_2$ group give rise to a singlet at 3.1 ppm. The $-\text{CH}_2$ group adjacent to the benzimidazole ring gives a doublet at 4.3 ppm due to coupling to the neighbouring amide NH proton while the $-\text{NH}$ between C=O and $-\text{CH}_2$ shows a triplet at 8.6 ppm due to coupling to the neighbouring $-\text{CH}_2$ protons [17,18] (Fig. 1 – Supplementary material).

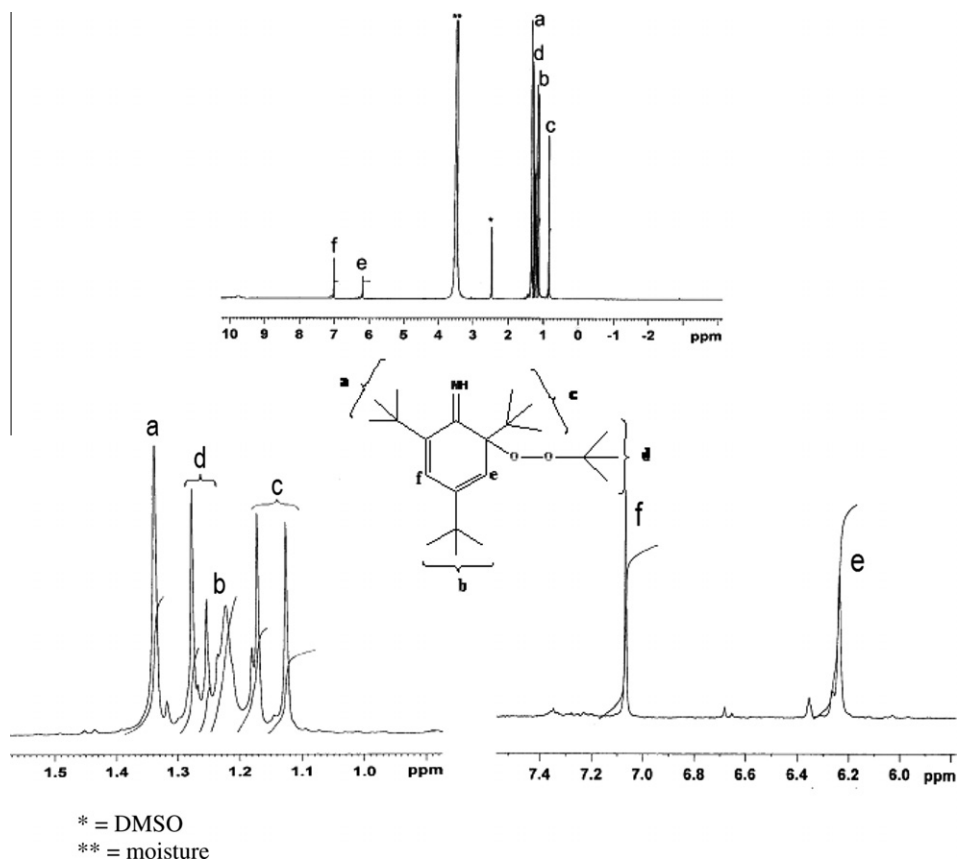


Fig. 3d. ^1H NMR in d_6 -DMSO of oxidation product of TTBA with $\text{Mn}(\text{L})\text{Cl}_2/\text{TBHP}$ and blow up of relevant region.

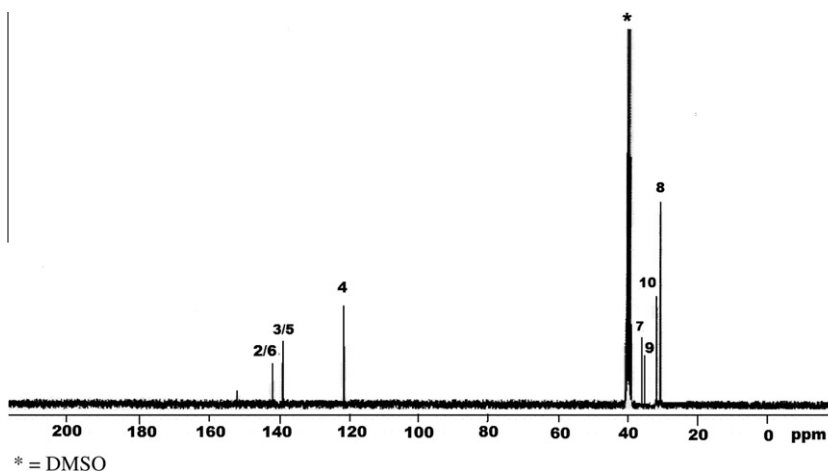


Fig. 4a. ^{13}C NMR in d_6 -DMSO of oxidation product of TTBP with $\text{Mn}(\text{L})\text{Cl}_2$ and H_2O_2 .

3.4. EPR Spectroscopy

X-Band EPR spectra of the Mn(II) complexes were obtained in the solid state at liquid nitrogen temperatures.

The spectra of $[\text{Mn}(\text{L})\text{Cl}_2]$, $[\text{Mn}(\text{L})(\text{SCN})_2]$ complexes reveal transitions in the 5000 Gauss scan. An intense transition is centred at $g \sim 2.0$ while medium to weak transitions are seen at $g \sim 2.3$, 4.0 and 4.8. This suggests axially distorted Mn(II) complexes in the above cases, which are predicted to give five $\Delta M_s = \pm 1$ fine structure tran-

sitions [19]. While the EPR spectra of $[\text{Mn}(\text{L})(\text{CH}_3\text{COO})_2]$ complex shows the presence of a strong signal in the $g = 2.0$ region. No other signal is observed in the 5000 Gauss scan spectra, as would have been expected for non-cubic Mn(II) – complexes with appreciable zero field splitting. Such a one line spectrum devoid of any hyper-fine structure has been interpreted as arising from a Mn(II) complex with a neighbouring atom magnetic interaction [20,21]. The parameter D has been evaluated following the method of Korteweg and Reijen [22] (Table 4 – Supplementary material).

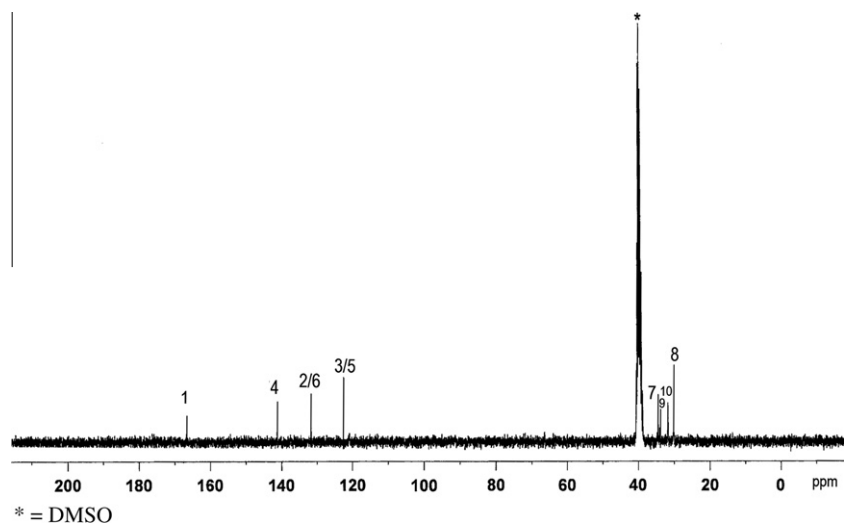


Fig. 4b. ^{13}C NMR in d_6 -DMSO of oxidation product of TTBA with $\text{Mn}(\text{L})\text{Cl}_2$ and H_2O_2 .

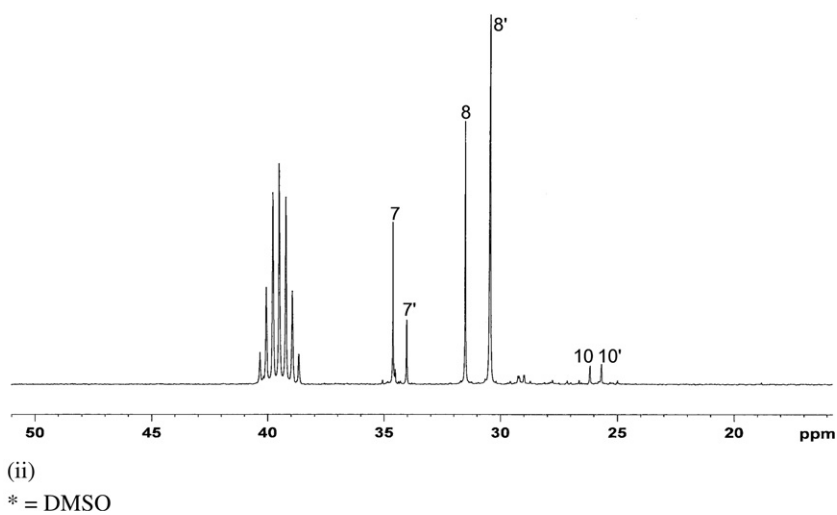
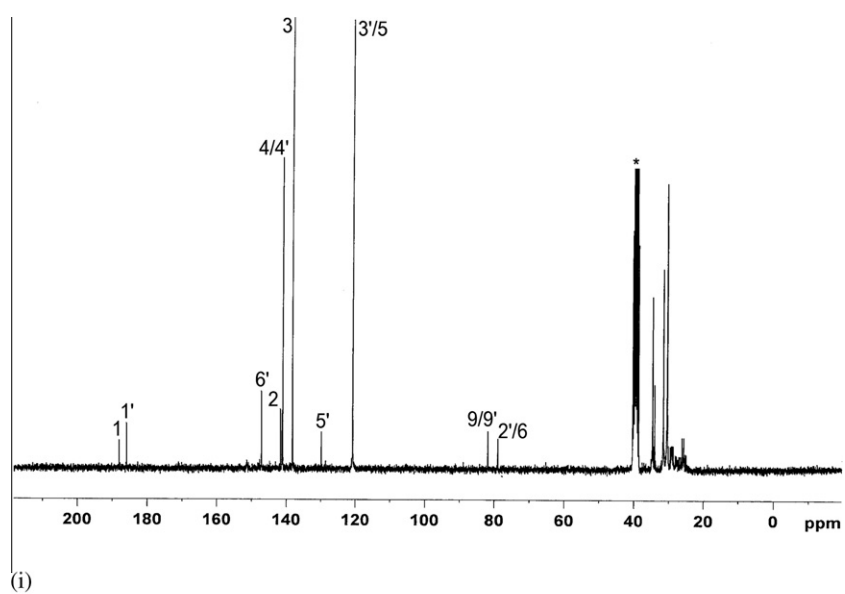


Fig. 4c. ^{13}C NMR in d_6 -DMSO of oxidation product of (i) TTBP with $\text{Mn}(\text{L})\text{Cl}_2$ and TBHP (ii) blow ups.

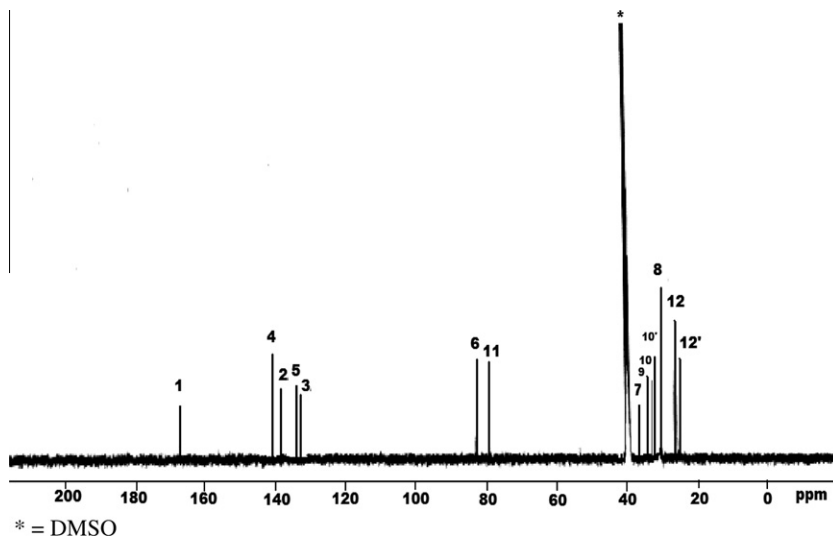


Fig. 4d. ^{13}C NMR in d_6 -DMSO of oxidation product of TTBA with $\text{Mn}(\text{L})\text{Cl}_2$ and TBHP.

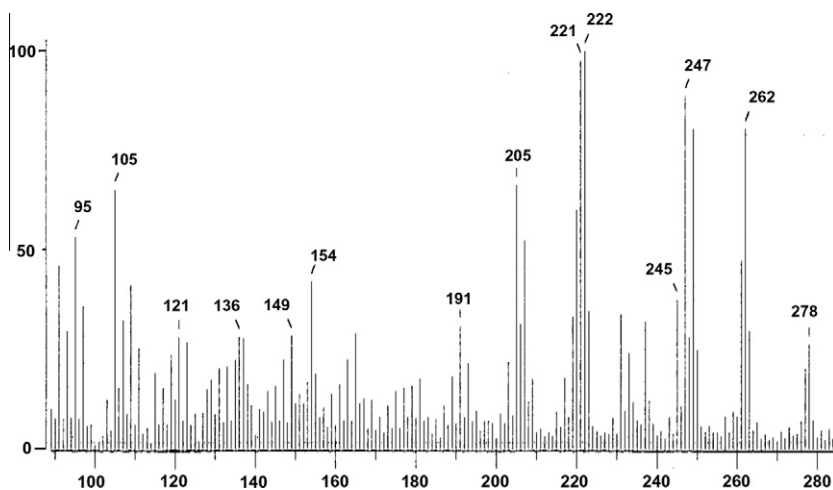


Fig. 5a. ESI mass spectra of oxidation product of TTBP + $\text{Mn}(\text{L})\text{Cl}_2$ + H_2O_2 .

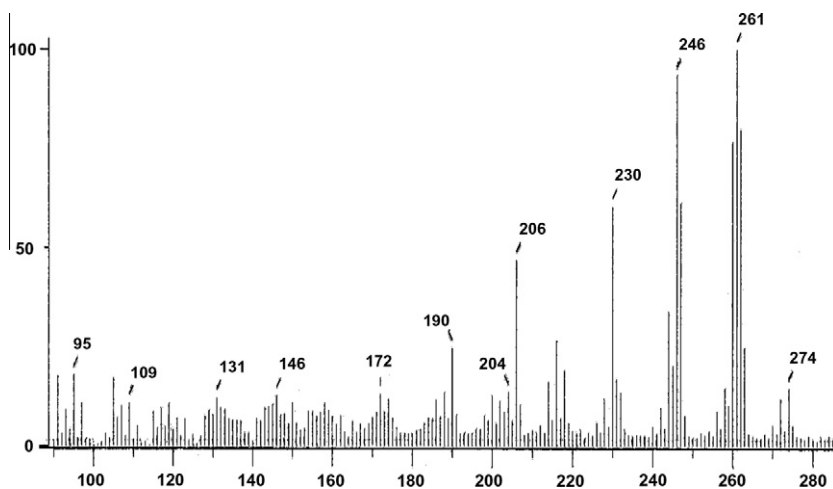


Fig. 5b. ESI mass spectra of oxidation product of TTBA + $\text{Mn}(\text{L})\text{Cl}_2$ + H_2O_2 .

3.5. Catalytic oxidation of hindered phenol (TTBP) and aniline (TTBA)

Stable oxidation products are generated during the catalytic oxidation of 2,4,6-tri-tert.-butylphenol and 2,4,6-tri-tert.-butylani-

line. IR spectra (in KBr) of products display bands in the region of $1640\text{--}1670\text{ cm}^{-1}$, confirming the presence of carbonyl group in them, and is also in keeping with a cyclohexadienone structure [23], the only exception is compound **B**.

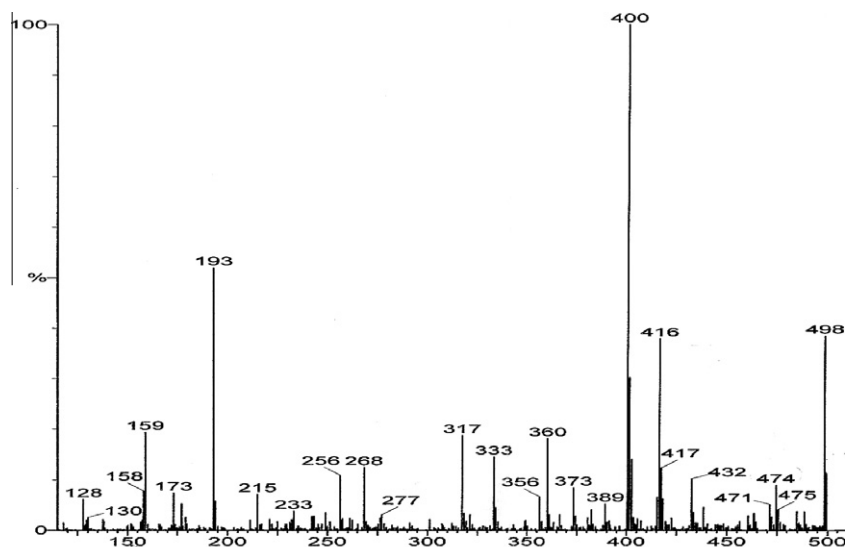


Fig. 5c. ESI mass spectra of oxidation product of TTBP + Mn(L)Cl₂ + TBHP.

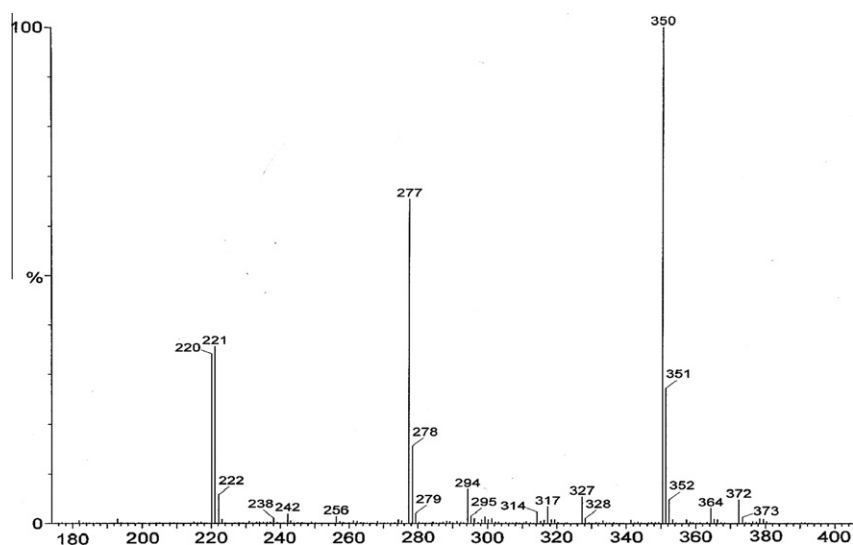
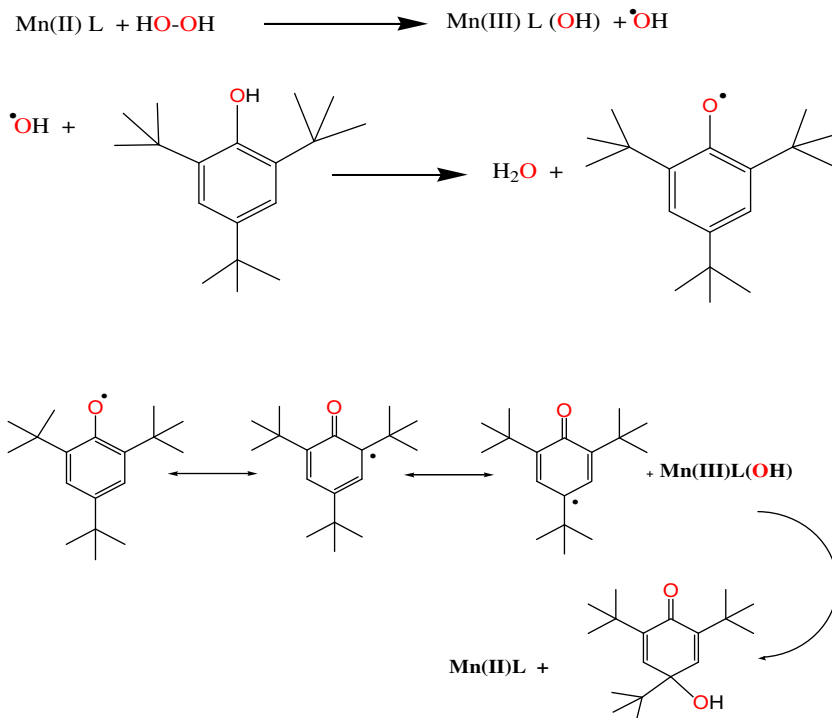


Fig. 5d. ESI mass spectra of oxidation product of TTBA + Mn(L)Cl₂ + TBHP.

¹H NMR spectrum of the product A in *d*₆-DMSO (Fig. 3ai) shows a singlet at 6.69 ppm which is assigned to the hydroxyl proton at para position. This is confirmed by performing a D₂O exchange experiment. Addition of D₂O to the sample in *d*₆-DMSO solution diminishes the peak at 6.69 ppm (Fig. 3a_{ii}). The peak at 7.09 ppm is due to C=CH protons and is assigned to protons associated with C3–C5 of the cyclohexadienone ring suggesting that the protons at C3–C5 are chemically equivalent as has been observed for para-cyclohexadienones [24]. The signals of the tert.-butyl protons are observed at 1.19 and 1.37 ppm, the relative integration ratios of the two peaks suggest that one of the tert.-butyl group is in a different chemical environment than the remaining two groups. In the ¹³C NMR (Fig. 4a), the signal of C1 (C=O) is expected to be at ~190 ppm but cannot be seen due to its weakness. The mass spectrum shows the following peaks 278 [M] (30%), 262 [M–(O)] (85%), 247 [M–(O+CH₃)] (80%), 222 [M + H–tBu] (100%), 221 [M⁺–(tBu)]. The ¹H NMR, ¹³C NMR and the fragmentation pattern observed in the mass spectra confirm the identity of product A (Scheme 1). Formation of such a hydroxy bound product has been proposed earlier also [6].

Product B is obtained by oxidation of 2,4,6-tri.tert.-butylaniline with hydrogen peroxide which leads to a nitrosobenzene derivative. This product does not show a strong band in the IR region of 1642–1677 cm⁻¹ excluding the possibility of a carbonyl group. The ¹H NMR (Fig. 3b) shows a single peak at 7.06 ppm suggesting that the protons at C3–C5 are equivalent [24]. The signals of the protons of tert.-butyl groups are found at 1.22 and 1.38 ppm, the relative integration ratios of the two peaks suggest that one of the tert.-butyl group is in a different chemical environment than the remaining two groups, suggesting a para substituted derivative. In the ¹³C NMR the C1 carbon carrying the NO absorbs at 168 ppm which is different from that of a carbon carrying the carbonyl group. The mass spectrum (Fig. 5b) shows the following peaks 274 [M–H] (20%), 261 [M–Me+H] (100%), 246 [M–2Me+H] (80%), 230 [M–3Me] (60%). The ¹³C NMR, base peak and other fragments confirm the identity of product B, formation of such a product has been postulated also earlier [16,9].

Product C is obtained by reaction of 2,4,6-tri.tert.-butylphenol with tert.-butylhydroperoxide, this leads to a >C–C< coupled product, supported by the mass spectrum that shows peaks at: 474 [M]



Scheme 1. Oxidation of hindered phenol using H_2O_2 as an oxidant.

(10%), 432 [M-(3Me)+3H] (12%), 416 [M-(CMe₃+H)] (38%) and 400 [M-(OCMe₃+H)] (100%), the higher peak at 498 is assigned to [M+Na⁺+H]; in its ¹H NMR spectra (Fig. 3c) two resonances are observed at 6.67 and 7.09 ppm assigned to the protons on C3'/5 and C3/5' on two ring system and are supported by their integral ratios. The tert.-butyl groups are observed at 1.17–1.19, 1.24 and 1.38 ppm. The integration ratios of their signals suggest that the two tert.-butyl groups attached to peroxyyl resonate at different positions, while the remaining two tert.-butyl groups are equivalent and resonate at the same position (blow up of the aliphatic region between 0.9 and 1.5 ppm has been provided).

The presence of a peak at 0.93 ppm is assigned to two hydrogen atoms at C4/4'. In the ¹³C NMR (Fig. 4c) two peaks are observed for C1 and C1' at 188 and 185 ppm confirming the presence of two carbonyl groups; the C7/7' carrying the tri methyl groups and C8/8' are found in the range of 33–35.5 and 30–31.0 ppm, respectively. The signals of C9/9', C2'/6 that are associated with peroxyyl group are found at 82 and 79 ppm, implying that these carbons are widely different from the carbons carrying the regular tri methyl group. Further it strengthens the presence of two tert.-butyl peroxyyl groups in the product C [16]. The presence of two sets of carbon-peaks in this molecule suggests that the two rings are not coplanar giving rise to an unsymmetrical structure¹. The above data justifies the C–C coupled product identified as C (Scheme 2).

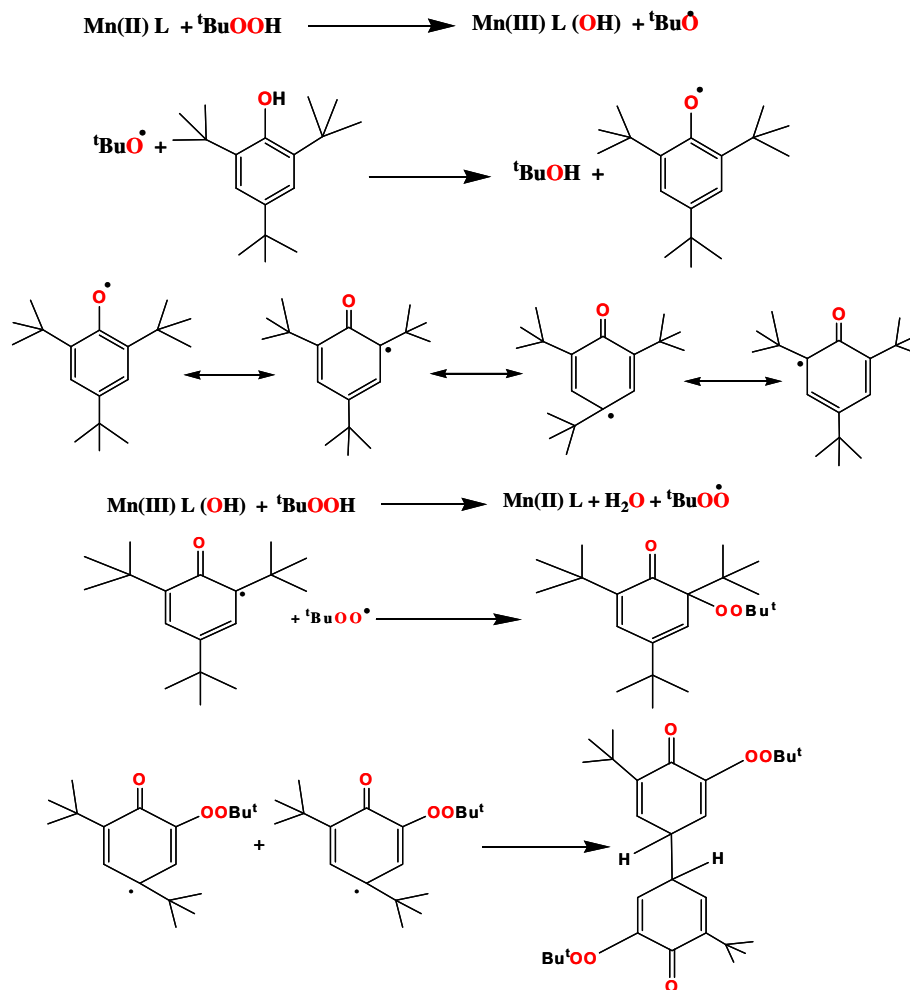
¹ In the context of product C, it is important to note that bianthrone (bis-tricyclic compounds with two carbonyl groups) relieve steric interactions by deviating from coplanarity and generate folded structures. Methyl substitution at 2,2' position permits the identification of two isomeric forms by ¹H NMR studies, and a doubling of signals have been observed; while substitution at 1,1' position leads to exclusive formation of one isomeric form [I. Agrat, Y. Taputi, *J. Org. Chem.* 12 (1979) 1941]. It is possible that compound C is a mixture of two isomers in a 1:1 ratio that may also account for the doubling of peaks in NMR. However as we are unable to resolve the isomeric forms (if they exist) we are proposing C as an unsymmetrical dimer.

Product D is obtained by oxidation of 2,4,6-tri-tert.-butylaniline with TBHP, its mass spectrum supports a cyclohexadiene type structure with a tert.-butylperoxy attached at the ortho position: 350 [M+H] (100%), 277 [M-OCMe₃+H] (66%), 220 [M-(OCMe₃+CMe₃+H)] (38%). The tert.-butyl groups in ¹H NMR (Fig. 3d) are observed at 1.17, 1.22, 1.25–1.27 and 1.33 ppm implying inequivalent tert.-butyl groups (blow up of the region 1.0–1.5 ppm has been provided, indicating the inequivalence of methyl groups)². While protons associated with C3/5 are observed at 6.21 and 7.09 ppm suggesting inequivalent C=CH protons. A broad band at 10.06 ppm is observed because of presence of NH in the product. This assignment is confirmed by performing a D₂O exchange experiment. Addition of D₂O to the sample in d₆-DMSO solution diminishes the peak at 10.06 ppm, and leaves the remaining peaks unchanged. Thus confirming that the peroxyyl group is at the ortho position. In the ¹³C NMR (Fig. 4d), peak at 166 ppm is observed for C1. Further peaks observed at 83 and 79 ppm are assigned to C4 and C9 carbon and are in keeping with the position of C9/9' and C2/6' found for the product C carrying the peroxyyl groups. However, the signals of C-12 and C-12' are split in contrast to the ¹H NMR signals. ¹³C NMR data are in keeping with an earlier report of such a peroxy bound product [16].

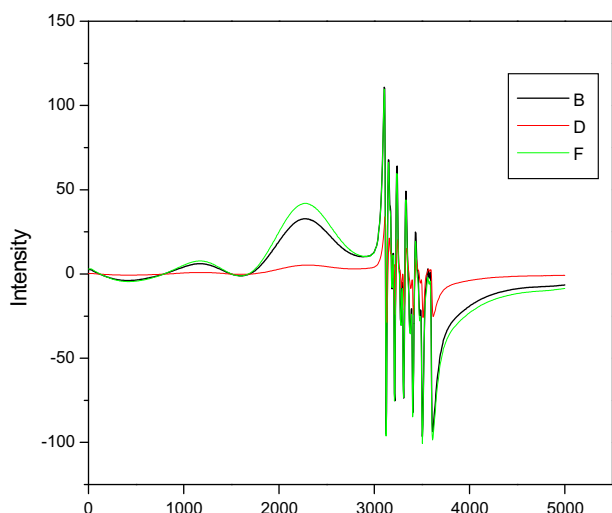
3.6. Monitoring of Mn catalyst by EPR Spectroscopy during oxidation reaction

The catalytic reaction between TTBP, catalyst Mn(L)Cl₂ and oxidant TBHP was monitored by time dependent EPR Spectroscopy at T = 100 K. In the blank experiment, three prominent signals are

² In the context of product D, it is interesting to note that the signal of two tert.-butyl groups split into two to three lines, which indicates that the tert.-butyl groups show hindered rotation. This has also been observed with other tert.-butyl groups at an sp³ center [L.M. Jackman, S. Sternhell, *Application of Nuclear Magnetic Resonance Spectroscopy in Organic Chemistry*, second ed, vol. 5, 1969].



Scheme 2. Oxidation of hindered phenol using TBHP as an oxidant.



Solutions	Area of $g \sim 2.95$ peak = $1/2 \times (\text{height of peak} \times \text{width of peak})$
[F]	437.5
[B] (0 min)	367.5
[D] (60 mins)	350.0

Fig. 6. X-Band EPR spectra of $\text{Mn(L)Cl}_2 + \text{TTBP}$ in methanol [F] $\text{Mn(L)Cl}_2 + \text{TTBP} + \text{TBHP}$ (0 min) [B] $\text{Mn(L)Cl}_2 + \text{TTBP} + \text{TBHP}$ (60 min) [D] at microwave frequency 9.4 GHz and receiver gain 10^3 .

observed when $[\text{Mn(II) complex}]$ was mixed with $[\text{TTBP}]$ at $g \sim 2.00$, $g \sim 2.96$ and $g \sim 6.00$ [trace F] (Fig. 6). On adding $[\text{TBHP}]$ it was found that all the transitions at $g = 2.0$, $g = 2.95$ and $g = 6.00$ undergo a diminishing in intensity and its overall area. A change of approx. 2.5 times in the area of peak centred at $g = 2.95$ is observed as the reaction proceeds in a catalytic manner to generate peroxy products [trace B and D]. The diminishing in the intensities of band is indicative of the formation of Mn(III) complex via oxidation of the starting Mn(II) catalyst.

Acknowledgements

We gratefully acknowledge financial support from the Defence Research Development Organization, Directorate of Extramural Research and Intellectual Property Rights, and special research grant from University of Delhi, Delhi, India.

We are also grateful to reviewers for their highly constructive suggestions.

Appendix A. Supplementary material

Supplementary data (^1H NMR of the ligand, geometry optimized structures and tables related to IR stretching frequencies, bond lengths along with EPR data of complexes) associated with this article can be found, in the online version, at [doi:10.1016/j.ica.2010.06.064](https://doi.org/10.1016/j.ica.2010.06.064).

References

- [1] C. Mantel, C. Baffert, I. Romero, A. Deronzier, J. Pecaut, M.-N. Collomb, C. Duboc, *Inorg. Chem.* 43 (2004) 6455.
- [2] B.A. Bernat, L.T. Laughlin, R.N. Armstrong, *Biochemistry* 38 (1999) 7462.
- [3] L. Requena, S. Bornemann, *Biochem. J.* 343 (1999) 185.
- [4] A.L. Schwartz, E. Yikilmaz, C.K. Vance, S. Vathyam, R.L. Koder, A.-F. Miller, J. *Inorg. Biochem.* 80 (2000) 247.
- [5] S.K. Smoukov, J. Telser, B.A. Bernat, C.L. Rife, R.N. Armstrong, B.M. Hoffman, *J. Am. Chem. Soc.* 124 (2002) 2318.
- [6] M. Frostin-Rio, D. Pujol, C. Bied-Charreton, M. Perree-Fauvet, A. Gaudemer, *J. Chem. Soc., Perkin Trans.* (1984) 1971.
- [7] L.I. Simandi, *Catalytic Activation of Dioxygen by Metal Complexes*, Kluwer Academic Publishers, Dordrecht, Boston, London, 1992. p. 196.
- [8] A. Nishinaga, S. Forster, E. Eichhorn, B. Speiser, A. Rieker, *Tetrahedron Lett.* 33 (1992) 4425.
- [9] J. Knaudt, S. Forster, U. Bartsch, A. Rieker, E.-G. Jager, *Z. Naturforsch.* 55b (2000) 86.
- [10] N. Kitajima, T. Koda, Y. Iwata, U.T. Moro-oka, *J. Am. Chem. Soc.* 112 (1990) 8833.
- [11] R. Gupta, R. Mukherjee, *Tetrahedron Lett.* 41 (2000) 7763.
- [12] M. Gupta, S.K. Upadhyay, M.A. Sridhar, P. Mathur, *Inorg. Chim. Acta* 359 (2006) 4360.
- [13] L.A. Cescon, A.R. Day, *J. Org. Chem.* 27 (1962) 581.
- [14] J.J.P. Stewart, *J. Comput. Chem.* 10 (1989) 221.
- [15] I.N. Levine, *Quantum Chemistry*, Prentice Hall, New Jersey, 2001.
- [16] S. Forster, K. Maruyama, K. Murata, A. Nishinaga, A. Rieker, *J. Org. Chem.* 61 (1996) 3320.
- [17] F. Afreen, P. Mathur, A. Rheingold, *Inorg. Chim. Acta* 358 (4) (2005) 1125.
- [18] M. Gupta, R.J. Butcher, P. Mathur, *Inorg. Chem.* 40 (5) (2001) 878.
- [19] R.H. Felton, L.D. Cheung, R.S. Philips, *S.W. Mag. Biochem. Biophys. Res. Commun.* 85 (1978) 844.
- [20] R.D. Dowsing, J.F. Gibson, M. Goodgame, P.J. Hayward, *J. Am. Chem. Soc.* (1969) 187.
- [21] A.V. Heuvelen, M.D. Lundeen, H.G. Hamilton, M.D. Alexander, *J. Chem. Phys.* 50 (1969) 489.
- [22] G.A. Korteweg, L.L. Van Reijen, *J. Magn. Reson.* 44 (1981) 159.
- [23] S.J. Valenty, G.L. Gaines, *J. Am. Chem. Soc.* 99 (4) (1977) 1287.
- [24] A. Nishinaga, H. Tomita, K. Nishizawa, T. Matsuura, *J.C.S. Dalton Trans.* (1981) 1504.